Engineering Failure Analysis 97 (2019) 464–479

Contents lists available at ScienceDirect

Engineering Failure Analysis

journal homepage: www.elsevier.com/locate/engfailanal

Lifetime wave overtopping risk analysis of sea defences subjected to changing operational conditions

Hua-Peng Chen[a,*], Mehrdad Bahari Mehrabani[b]

[a] Engineering Research Centre of Railway Environmental Vibration and Noise, East China Jiaotong University, Nanchang 330013, China
[b] Department of Engineering Science, University of Greenwich, Chatham, Kent ME4 4TB, UK

ARTICLE INFO

Keywords:
Sea defence
Wave overtopping
Sea level rise
Stochastic deterioration modelling
Risk analysis
Maintenance strategy

ABSTRACT

Sea defences are at increasing risk of wave overtopping due to changing hydraulic conditions caused by climate change and deteriorating structural resistance. This paper presents a method for assessing wave overtopping risk of coastal flood defences subjected to changing operational conditions. The joint probability of hydraulic parameters such as sea water level and significant wave height is investigated using the extreme value analysis approaches taking into account rising sea level in the future. Meanwhile, structural resistance degradation such as the crest level settlement of earth sea dykes is considered in overtopping risk analysis by utilising a state-based stochastic deterioration model. Time-dependent probability of wave overtopping failure is estimated from the associated limit state equation, and the effect of hydraulic parameters and crest level settlement on the risk of overtopping failure is investigated. A risk cost optimised maintenance strategy is then determined by balancing the risk of overtopping failure and the costs for structural maintenances. The results for the numerical example of a typical earth sea dyke show that the probability of overtopping failure will increase significantly due to changing hydraulic parameters and losing crest level, thus appropriate maintenance will be needed to reduce the risk during the lifecycle.

1. Introduction

Sea defences provide essential protection against flooding and coastline erosion, thus they are required to perform well and operate reliably during the service life. However, the influence of hydraulic conditions caused by changing environments, such as sea level rise, may reduce the performance of the structures in the future. The future rise in sea level was projected in global scale by Intergovernmental Panel on Climate Change (IPCC) [1] and in national scale by the United Kingdom Climate Projection (UPCP) [2], subject to various emission scenarios till the end of this century. Sea level rise may lead to storm amplification and higher wave heights, and also increase in the number of extreme events [3]. Hallegatte et al. demonstrated that the magnitude of loss and damage in coastal cities due to the increase in the future floods could increase > 50% by 2050, since the severity and frequency of the floods will increase due to sea level rise [4]. Bosello and De Cian showed that without adaptation to the projected sea level rise, 12% of lands in Europe continent will be sunk by the end of this century, while the loss could be reduced > 85% by increasing the protection in flood defence structures [5]. Meanwhile, the deterioration of the coastal flood defences, such as crest settlement over time, will reduce structural resistance, leading to increase in probability of failure of the structure. Hence, it is crucial to manage the risk of future flooding through appropriate risk analysis and optimal maintenance strategies with consideration of changing operational

* Corresponding author at: School of Civil Engineering and Architecture, East China Jiaotong University, Jiangxi 330013, China.
E-mail addresses: hp.chen@ecjtu.edu.cn, hp.chen@outlook.com (H.-P. Chen).

https://doi.org/10.1016/j.engfailanal.2019.01.037
Received 18 June 2018; Received in revised form 12 October 2018; Accepted 3 January 2019
Available online 07 January 2019
1350-6307/ © 2019 Elsevier Ltd. All rights reserved.

conditions.

Wave overtopping failure is often considered as an indicator for the serviceability performance level of coastal flood defences. Wave overtopping is mainly caused by the joint effect of hydraulic parameters such as sea water level and significant wave height. Hence, the joint probability of these hydraulic parameters is needed to be investigated. Hawkes et al. introduced joint probability methods for flood and coastal defences and applied these methods in several case studies, where many statistical models and various fitting techniques were described [6]. Chini and Stansby proposed a method for joint extreme value analysis between sea water level and significant wave height subjected to sea level rise, in order to predict wave overtopping in the future [7]. It is shown that the frequency and magnitude of extreme wave overtopping discharge will increase significantly with time, depending on future climate projections and sea level rise. These methods provide further understanding of the joint probability analysis for quantitative risk analyses of wave overtopping affected by the future hydraulic conditions.

On the other hand, deterioration of coastal flood defences poses a significant challenge in the asset management, since the deterioration leads to decreasing in resistance of the structures. Structural resistance deterioration, such as crest settlement, may significantly influence the reliability of coastal flood defences during the lifecycyle. In order to accurately analyse the lifetime structural reliability, stochastic deterioration models have been developed and utilised for various civil engineering structures such as bridges [8]. Baik et al. proposed a Markov model for wastewater systems to predict the future performance deterioration of the systems using available inspected data [9]. Saydam et al. adopted a homogeneous Markov process for estimating the transition probabilities between the condition states to investigate the deterioration process of bridge components [10]. In addition, many studies have been carried out on the performance prediction and maintenance strategies of coastal flood defences, including time-dependent reliability analysis [11], and reliability-based maintenance [12]. Chen proposed a method for reliability analysis of existing coastal defences associated with wave run-up and overtopping under future hydraulic conditions [13]. An approach for optimising the expected maintenance costs and inspection time interval was then proposed by using a renewal maintenance model [14]. However, there is still limited research available on time-dependent reliability analysis of existing coastal defence systems affected by future hydraulic loading conditions and structural resistance deterioration. There is therefore a need to develop an effective tool for analysing lifetime reliability of sea defences with consideration of changing operational conditions.

This paper proposes a new approach for predicting future wave overtopping performance of sea defences with consideration of changing hydraulic conditions and decreasing structural resistance. From the collected and projected data, the joint probability of water level and wave height is analysed for the present and future hydraulic conditions. The state-based stochastic deterioration model such as Markov process is employed for modelling structural resistance deterioration such as crest height settlement over time. The transition probability over time of the stochastic deterioration model is estimated on the basis of available deterioration curves obtained from routine inspections. The probability of wave overtopping failure of the deteriorating sea defences is then calculated from the associated limit state equation taking into account future hydraulic conditions and resistance deterioration. Finally, a numerical example for an earth sea dyke section is employed to demonstrate the applicability of the proposed approach for predicting future wave overtopping risk of the sea defence. The results show that the proposed method can give lifetime overtopping risk of deteriorating coastal flood defences and provide a tool for determining risk-cost optimised maintenance strategies.

2. Hydraulic parameters for wave overtopping

Sea defences are designed to service for a long period, and changes in initial hydraulic conditions often occur in practice. The future hydraulic loads on the structures can be affected by rising sea level and varying wave parameters due to climate change [7]. This may lead to increase of the coastal flooding risk and decrease of the reliability of coastal flood defences.

2.1. Sea level rise and wave height change

The projection of rising sea level in the UK has been reported in UKCP09 [2] on the basis of various greenhouse emission scenarios, i.e. low, medium and high emission scenarios. The range with 5th to 95th percentile confidence intervals of absolute sea level rise around the UK before consideration of vertical land movements is projected for the future, depending on emission scenarios. The absolute sea level changes and vertical land movements are then combined into estimates of relative sea level rise, which is used

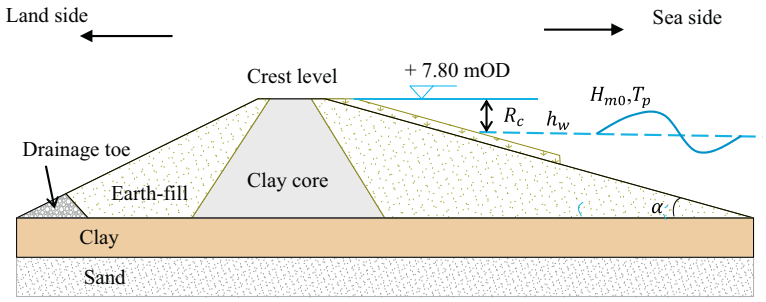

Fig. 1. Sketch of an earth sea dyke section of Thames Estuary flood defence systems.

in this study.

Sea level rise will increase the wave attack on coastal flood defences such as earth sea dykes, as shown in Fig. 1, if local wave heights are depth-limited [14]. Due to the limited depth, waves may break when they reach a relatively shallow foreshore at the toe of the dyke seaside slope. The depth-limited spectral significant wave height $H_{m0}(t)$ over time t depends on many factors including still water level at the toe of the sea defence. The local water level $h_w(t)$ at the toe increases with time t due to sea level rise $\Delta h_w(t)$, expressed here as

$$h_w(t) = h_w(0) + \Delta h_w(t) \tag{1}$$

where $h_w(0)$ represents the present water level associated with the design water level at a chosen return period. From the energy decay numerical model for uniform foreshore slopes by Van der Meer et al. [15] in which the influence of wave breaking is considered, the depth-limited significant wave height $H_{m0}(t)$ is estimated from hydraulic conditions including deep-water wave steepness S_{op} and local relative water depth $h_l(t)$ together with foreshore slope. The increasing local water depth due to sea level rise affects the local relative water depth, which has an impact on the depth-limited significant wave height. Here, the local relative water depth over time $h_l(t)$ is defined here as

$$h_l(t) = \frac{h_w(t)}{L_{op}} \tag{2}$$

where peak wave length L_{op} is related to peak wave period T_p, estimated from

$$L_{op} = \frac{gT_p^2}{2\pi} \tag{3}$$

where g is the acceleration due to gravity. The deep-water wave steepness S_{op} is calculated from deep-water significant wave height H_{so} over peak wave length L_{op}, namely

$$S_{op} = \frac{H_{so}}{L_{op}} \tag{4}$$

Thus, the depth-limited significant wave height $H_{m0}(t)$ due to rising sea level over time can be estimated if the wave parameters together with the deep-water significant wave height are available. The change in wave periods due to climate change is negligible [3] and is not considered in this study.

2.2. Joint probability of water level and wave height

Wave overtopping discharge over a sea defence depends largely on two main hydraulic parameters acting on the structure, e.g. water level and wave height. Here, these two hydraulic parameters, water level and wave height, are considered as random variables in joint probability analysis. Estimation of the joint probability of these two random variables has been investigated in many studies [7,16]. In the cases where more than two random variables are considered in the joint probability, a direct extension of that for the two random variables should be undertaken. In this study, the joint occurrence associated with the return period T_r of the extreme values of water level and significant wave height is considered. There are several approaches available for extreme value analyses for marginal distributions in joint probability evaluation, such as Generalised Extreme Value (GEV) distribution and Generalised Pareto Distribution (GPD).

The GEV distribution is a family of continuous probability distributions combining three asymptotic forms of extreme value distributions, Gumbel, Weibull and Fréchet [17]. The cumulative density function for the GEV distribution with respect to random variable x is rewritten here as

$$F(x) = \exp\left[-\left\{1 + \kappa\left(\frac{x-\mu}{\sigma}\right)\right\}^{-1/\kappa}\right] \tag{5}$$

where $\kappa \neq 0$, μ and σ are shape, location and scale parameters, respectively. The GEV distribution is the limit distribution of properly normalised maxima of a sequence of independent and identically distributed variables. Hence, the distribution is often used as an approximation to model the block maxima (e.g. annual maxima) for sequences of random variables such as water level and wave height.

The peak over threshold is an alternative approach for estimating extreme values from data over a specific threshold, for which the values may follow the GPD distribution [17]. The cumulative density function for the GPD distribution is rewritten here as

$$G(x) = 1 - \left[1 + \frac{\kappa(x-u)}{\sigma}\right]^{-1/\kappa} \tag{6}$$

where the threshold u is selected by utilising expected exceedance method through mean residual life plot. The parameters of the GEV and GPD distributions can be estimated using the maximum likelihood estimation method. In order to combine the marginal distributions and evaluate dependence structures, a copula function C is introduced to represent a multivariate probability distribution for which the marginal probability distribution of each variable is uniform [16]. Assuming cumulative distribution functions $F_1(x_1)$ and $F_2(x_2)$ to map generic random variables x_1 and x_2 into random variables $U_1 = F_1(x_1)$ and $U_2 = F_2(x_2)$, the copula of random

variables x_1 and x_2 is defined as the cumulative distribution function of U_1 and U_2 [18], expressed here as

$$C(u_1, u_2) = \Pr[u_1 \geq U_1, u_2 \geq U_2] \tag{7}$$

In the cases for assessing wave overtopping of sea defences, the water level and significant wave height are considered as two generic random variables. The joint distribution of water level h_w and significant wave height H_{m0} can then be expressed as

$$H(h_w, H_{m0}) = C(F_{h_w}(h_w), F_{H_{m0}}(H_{m0})) \tag{8}$$

The copula function C describes the dependence between sea water level and significant wave height that may be fitted either in the GEV or GPD distribution. Here, the Gumbel Archimedean copulas model is adopted to estimate the dependence value, as described in [18]. The joint exceedance $E_r(h_w, H_{m0})$ of sea water level h_w and significant wave height H_{m0} can now be expressed as

$$E_r(h_w, H_{m0}) = 1 - F_{h_w}(h_w) - F_{H_{m0}}(H_{m0}) + H(h_w, H_{m0}) \tag{9}$$

and the corresponding joint return period value $T_r(h_w, H_{m0})$ is given as

$$T_r(h_w, H_{m0}) = \frac{1}{\lambda_j E_r(h_w, H_{m0})} \tag{10}$$

where is λ_j the mean number of events per year.

3. State-based deterioration model

Routine inspections for civil engineering structures such as sea defences provide essential information about the performance level (e.g. condition grade) of the structures. Here, a stochastic process such as Markov process is employed to translate the condition grades at certain times into quantitative deterioration models, and these models are then used for time-dependent reliability analysis of the deteriorating sea defences.

3.1. Condition grade systems

In practice, a standardised framework for assessing structural condition and assisting decision making is often available for routine inspections, such as the condition assessment manual for flood defences published by Environment Agency in the UK [19]. According to this manual, the condition grading of the flood defence assets is represented by using numeric value of 1 to 5, as described in Table 1. In this grading system, Condition Grade 1 denotes the best condition and Grade 5 denotes the worst condition. The generic description of Grade 1 is that the assets are in good condition and there may be presents of superficial but not critical damage, while Grate 5 denotes that the asset is no longer able to perform its function at even a reduced level.

In addition, quantitative assessment methods are often adopted to improve asset condition assessment based on inspection strategy, expert judgment and simplified performance indicators [20]. The quantitative assessment approaches suggest that assets should be ranked according to their performance, general conditions and risk posed specifically. In fact, an asset is ranked based on the intensity and magnitude of damage, where slight damage, minor damage and major damage could correspond to condition Grade 1, Grades 2–3, and Grades 4–5, respectively. The quantitative approaches are used to link between structural damage and its relevant failure modes. The detailed dimensions of damage associated with their visual indicators and locations in an asset are available in Long et al. [20].

3.2. Stochastic deterioration modelling

In order to translate the condition grades over time into quantitative deterioration models, a stochastic process such as Markov process is employed. Markov process is a discrete-time stochastic time-dependent process for estimating the future events as a random outcome. Markov process is a suitable model for a state-based approach, and has been extensively used for predicting future condition of civil infrastructure systems [9,10].

In probability theory, a stochastic process has the Markov property if the conditional probability distribution of future states of the process, given the present state and all past states, depends only upon the current state and not on any past states. This property can be expressed for a discrete parameter stochastic process $S = \{s_n; n = 1, 2, \ldots\}$ with discrete state spaces [21], expressed here as

Table 1
Condition grades and descriptions adopted by UK Environment Agency.

Condition grade (CG)	Rating	Description
1	Very Good	Cosmetic defects that will have no effect on performance.
2	Good	Minor defects that will not reduce the overall asset performance.
3	Fair	Defects that could reduce performance of the asset.
4	Poor	Defects that would significantly reduce the performance of the asset.
5	Very poor	Severe defects result in complete performance failure.

$$p_{ij} = \Pr[s_n = i_n \mid s_{n-1} = i_{n-1},..., s_1 = i_1] = \Pr[s_n = i_n \mid s_{n-1} = i_{n-1}] \tag{11}$$

where i is the state of the process at time period n and p_{ij} is the conditional probability of any future event given the present and past events. When the Markov chain is used to model deterioration of a system in state i, a fixed probability exists so that the system will change from state i to state j during the next period. These probabilities p_{ij} are commonly represented by a matrix with dimensions of $M \times M$, called transition probability matrix (**P**) of the Markov chain, where M is the number of possible condition states. The general form of transition matrix **P** is given as

$$\mathbf{P} = \{p_{ij}\}_{M\times M} \tag{12a}$$

$$p_{ij} \geq 0 \text{ and } \sum_{j=1}^{M} p_{ij} = 1 \text{ for } i, j = 1, 2, ...M \tag{12b}$$

Each element p_{ij} in the transition probability matrix **P** represents the probability that the condition of a structural system or its component will move from state i to state j during a certain period of time, and the sum of the each row of the transition probability matrix is equal to one from total probability theorem.

For the cases for the condition assessment of flood defences by Environment Agency [19], the deterioration of the assets with progress of age is represented by five different condition grades (CG1 to CG5). The initial state of the structure, i.e. at time t=0, is represented by Grade 1 (CG1), and Grade 5 (CG5) represents the worst. If no rehabilitation or repair work has been carried out, the flood defence assets will be gradually deteriorating and hence their corresponding condition state will either upgrade to a higher grade number or remain unchanged during the inspection period. Hence, the probability p_{ij} in Eq. 12(a) is null for $i > j$ where i and j are aforementioned condition state of the Markov chain. Furthermore, the deterioration process is assumed to be unidirectional. This means that transition of condition grade would not be upgraded by more than one state within one unit period, hence the probability of upgrade to more than one state is zero. Consequently, the transition probability matrix **P** is reduced to an upper triangular diagonal transition matrix, simplified for UK Environment Agency grating systems as

$$\mathbf{P} = \begin{bmatrix} p_{11} & 1-p_{11} & 0 & 0 & 0 \\ 0 & p_{22} & 1-p_{22} & 0 & 0 \\ 0 & 0 & p_{33} & 1-p_{33} & 0 \\ 0 & 0 & 0 & p_{44} & 1-p_{44} \\ 0 & 0 & 0 & 0 & 1 \end{bmatrix} \tag{13}$$

The Markov process is stationary if the transition probability between the states is stationary for the same period of time step. The probability that a process in state i will be in state j after n transitions is defined as n-step transition probability. By using the matrix multiplication rule, the n-step transition probability matrix $\mathbf{P}_n$ is obtained by taking nth power of the one-step transition probability **P**, i.e. $\mathbf{P}_n = \mathbf{P}^n$.

To meet the homogeneity assumption of Markov chain, a zoning concept may be applied. A zone is a certain period of time assumed to produce constant transition probabilities, and the period for the zone is based on engineering judgment or inspection intervals [9,22]. The transition probability matrix **P** for n transitions is obtained by minimising the difference between the observed and predicted condition states of the asset, given as

$$\min_{p_{ij}} \sum_{k=1}^{K} \|\mathbf{B}_k - \mathbf{C_0}\mathbf{P}_{n_k}\mathbf{S}\| \tag{14}$$

The above optimisation problem is subject to constraints given in Eq. 12(b). Here $\mathbf{B}_k$ is observation of a condition grade at time-step n_k; K is the total number of observations; $\boldsymbol{S}$ is condition rating vector with $\boldsymbol{S} = [1\ 2\ 3\ 4\ 5]^T$ for the cases of UK Environment Agency grating systems [19]; $\boldsymbol{C}_0$ is the initial condition state probability vector at time zero, by assuming that newly constructed asset is defect free, giving a condition state probability of $\boldsymbol{C_0} = [1\ 0\ 0\ 0\ 0]$.

After the transition probability matrix is obtained, the probability distribution of condition grades at time t with n_t transitions is given as

$$\mathbf{C}(t) = \mathbf{C_0}\mathbf{P}^{n_t} \tag{15}$$

The probability distribution of condition grades over time indicates the asset condition deterioration with time by increasing the probability of upgrades, e.g. upgrading from CG1 to CG5.

4. Overtopping failure probability

Wave overtopping is the critical response of coastal flood defences such as earth sea dykes. Research showed that overtopping is a dominant failure mechanism with significantly increasing failure probability over time [14]. Excessive wave overtopping discharge causes erosion of landside slope and weakens soil shear strength due to saturation of slope soils. Due to varying hydraulic conditions caused by climate change, sea water level and significant wave height acting on the earth dyke are increasing with time. In the meantime, structural resistance of earth dykes is deteriorating with time, such as long-term settlement at dyke crest level. Consequently, the future freeboard representing the height of the structure crest above still water level will be reduced over time, leading to increasing in wave overtopping discharge in the future. On the basis of the limit state equation associated with wave overtopping, the

Table 2
Vertical crest level loss and probability density function assumed for earth dykes.

Condition grade (CG)	Crest level loss (m) [21]	Probability density function
1	0.00–0.05	Lognormal
2	0.05–0.10	Normal
3	0.10–0.20	Normal
4	0.20–0.40	Normal
5	0.40+	Lognormal

time-dependent failure probability can be estimated, which can be further used for optimising maintenance strategy for the sea defences.

4.1. Reduced crest freeboard over time

Wave overtopping rate of existing sea dykes mainly depends on crest freeboard available. The future freeboard $R_c(t)$ over time t is defined as the height of the dyke crest above still water level at the toe, and is affected by sea level rise $\Delta h_w(t)$ and earth sea dyke settlement $\Delta h_d(t)$, expressed here as

$$R_c(t) = R_c(0) - \Delta h_w(t) - \Delta h_d(t) \tag{16}$$

where $R_c(0)$ is initial freeboard at present day, and $\Delta h_d(t)$ is the deterioration of crest level in vertical direction at time t. During field condition assessment, the vertical crest level loss of earth dykes can be evaluated and then the condition state associated with the crest level loss can be assigned.

The suggested condition grades for the crest level loss are given in Long et al. [20], as listed in the second column of Table 2. The

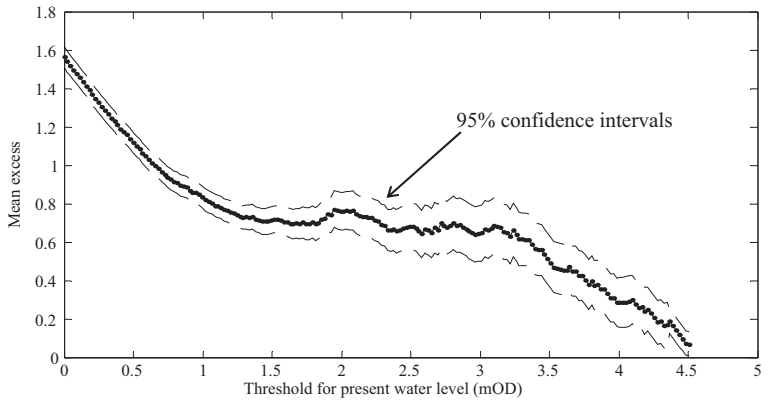

(a) Present sea water level

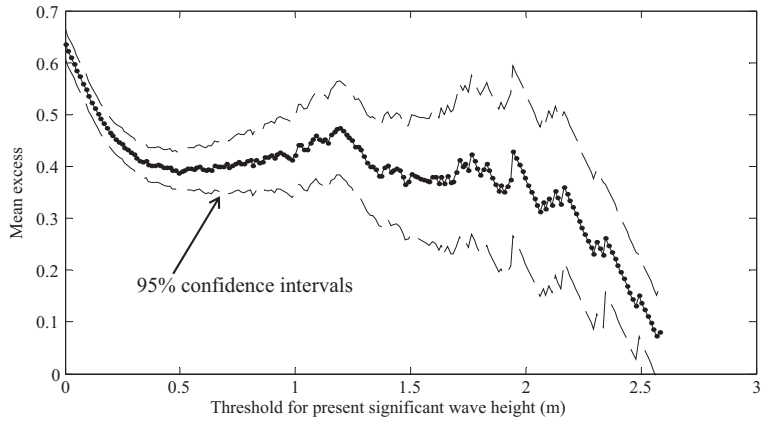

(b) Present significant wave height

Fig. 2. Mean excesses for sea water level and significant wave height at present day with 95% confidence intervals.

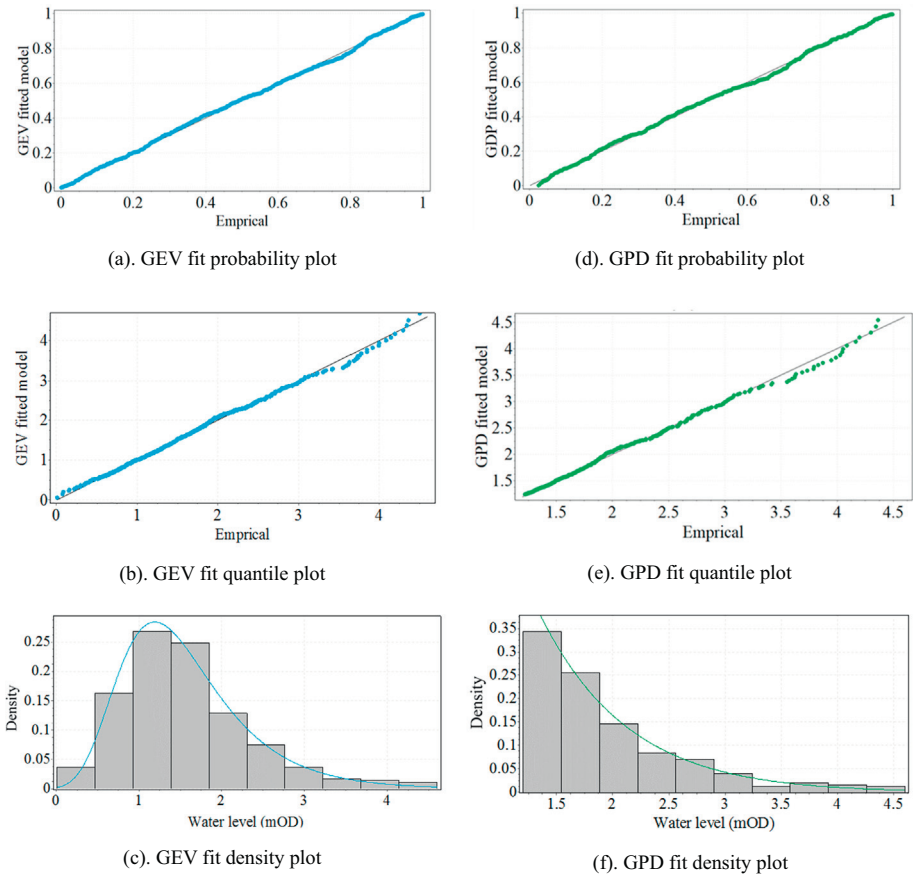

Fig. 3. Diagnostic plots for the GEV and GPD models fitted to the present water level dataset.

values for each condition grade can be adjusted if a site-specific investigation is undertaken. Here, the vertical dyke crest level loss for each grade is assumed to have a lognormal probability density function (PDF) for the highest and lowest condition grades CG1 and CG5, and a normal PDF for other condition grades, i.e. CG2, CG3 and CG4, as shown in Table 2. Here, the distributions for the condition grades CG1 and CG5 are assumed to be lognormal to reflect that the crest level will not increase due to structural deterioration with time for CG1 and that the negative crest level for the earth dyke is not possible for CG5. With consideration of uncertainty in field assessment, the deterioration intensities for the condition grades CG2, CG3 and CG4 are assumed to be normally distributed. To ensure these distributions are conservative, it is also assumed that the crest level is initially in the middle of a specific condition grade and progressively shifts to the right of the distribution with time. The mean value of the PDFs is taken as the average of the upper and lower limits of the crest level loss range, and the standard deviation is determined depending on the accuracy and confidence of the field inspection strategy. For the condition assessment undertaken by experts, the standard deviation could be chosen so that the cumulative probability between two limits of the crest level loss range is taken as an appropriate value reflecting data accuracy, e.g. approximately 90%.

Consequently, from the obtained current condition grade distribution $\mathbf{C}(t)$ at time t in Eq. (15), the earth dyke settlement over time is calculated from

$$\Delta h_d(t) = \sum_{m=1}^{M} C_m(t)\Delta l_m \tag{17}$$

where Δl_m is the vertical dyke crest level loss for the mth condition grade, which can be taken from the probability density function associated with the condition grade by Monte Carlo simulations. Once the vertical dyke crest level loss is available, the crest freeboard over time is then calculated from Eq. (16), and wave overtopping discharges over time can be predicted by empirical equations [23,24].

4.2. Limit state equation

In time-dependent reliability analysis, a limit state equation for a potential failure mechanism is needed to describe the resistance with time and the loads with time for the failure mode concerned [11,25–27]. Here, the failure caused by wave overtopping over time is defined as the exceedance of a predefined mean overtopping discharge q_{cr}, and the limit state equation for the wave overtopping

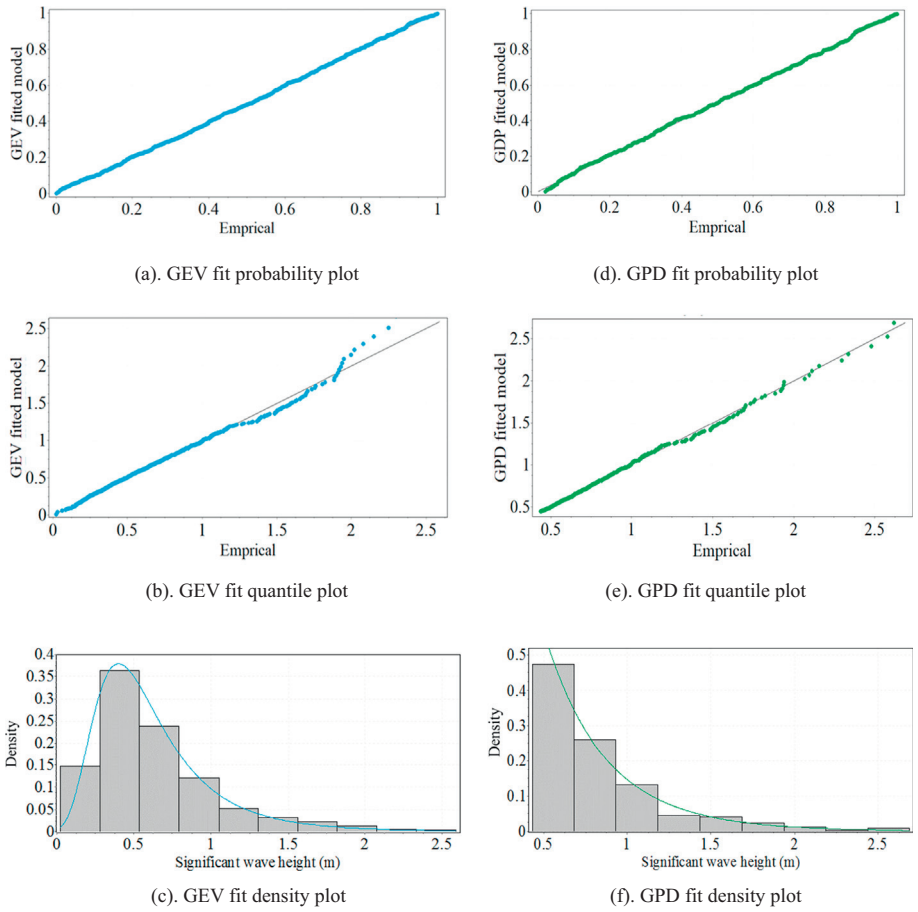

Fig. 4. Diagnostic plots for the GEV and GPD models fitted to the present significant wave height dataset.

failure mode is expressed as

$$Z_q(t) = q_{cr} - \chi_q q(t) \tag{18}$$

where χ_q is model uncertainty coefficient to account for uncertainties in input parameters for estimating overtopping discharge, such as wave height, wave period, water depth and slope angle of foreshore, and may be assumed to be normally distributed with a mean value of unity [14,23]; $q(t)$ is average overtopping discharge at time t, estimated from [14].

$$\frac{q(t)}{\sqrt{gH_{m0}{}^3(t)}} = \frac{B_1}{\sqrt{\tan\alpha}}\gamma_b\xi_{m-1,0}\exp\left[-\left(B_2\frac{R_c(t)}{\gamma_b\gamma_f\gamma_\beta\xi_{m-1,0}H_{m0}(t)}\right)^\tau\right] \tag{19a}$$

with a maximum of

$$\frac{q(t)}{\sqrt{gH_{mo}{}^3(t)}} = B_3\exp\left[-\left(B_4\frac{R_c(t)}{\gamma_f\gamma_\beta H_{mo}(t)}\right)^\tau\right] \tag{19b}$$

where $B_1 = 0.023$, $B_2 = 2.7$, $B_3 = 0.090$, $B_4 = 1.5$ and $\tau = 1.3$ are empirical coefficients; γ_b, $\gamma_f$and γ_β are correction factors for berm, roughness and oblique wave attack, respectively; and $\xi_{m-1,\,0}$ is local breaker parameter related to the slope steepness tanα.

In this study, Monte Carlo methods are utilised to generate values for the vertical dyke crest level loss for each condition grade at a certain time. These simulated crest freeboard values are then used for estimating the wave overtopping rates given in Eq. (19). By using the limit equation described in Eq. (18), the probability of failure is calculated from the number of failures generated in the simulations, since the Monte Carlo simulation method is a type of sampling procedure [14]. Once the failure probability $p_f(t)$ at time t is obtained, the probability of failure per unit time at the ith time interval is calculated from

$$p_i = p_f(t_i) - p_f(t_{i-1}) for\ i = 1,\ 2,\ 3... \tag{20}$$

where the time interval may be taken as one year for the convenience in calculations.

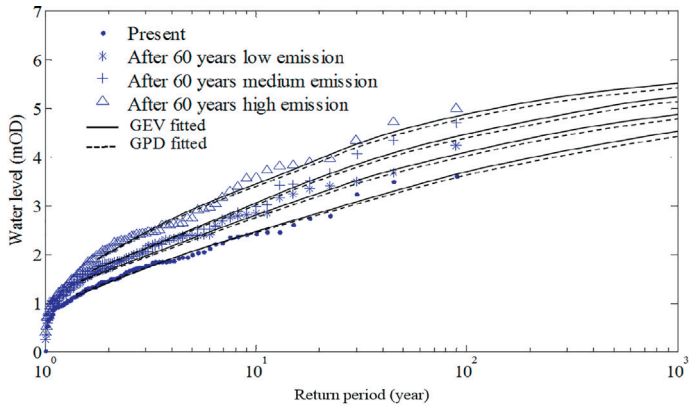

(a) Fitted models for sea water level

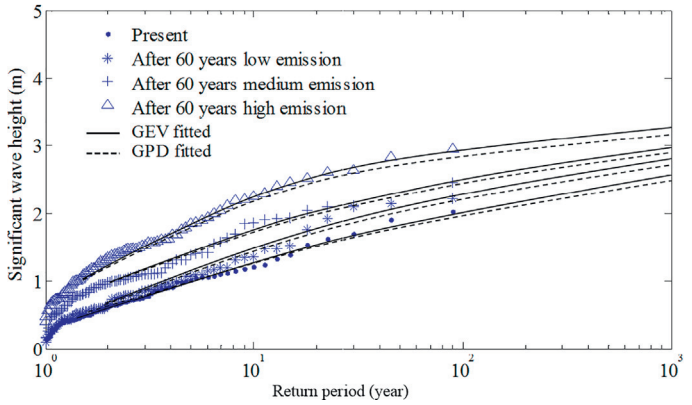

(b) Fitted models for significant wave height

Fig. 5. Return periods of the GEV and GPD fitted models for hydraulic parameters at present day and after 60 years subject to various emission scenarios.

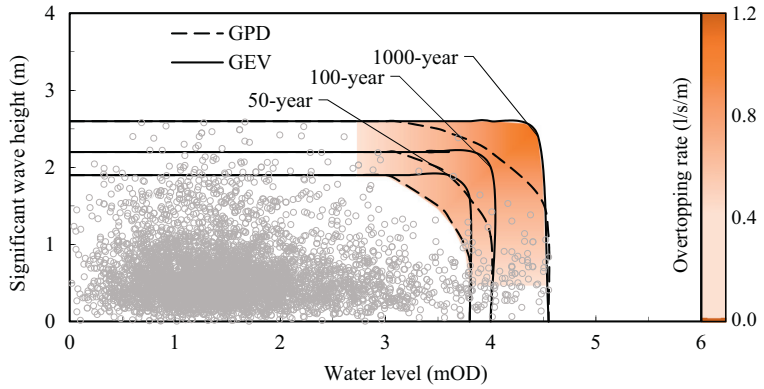

Fig. 6. Joint exceedance for sea water level and significant wave height under different return periods at present day.

4.3. Optimised maintenance strategy

Condition-based maintenance is undertaken at times determined by assessing a system's condition that can be evaluated by stochastic deterioration modelling [28,29]. Maintenance models typically use cost-based criteria such as the expected average cost per unit time. The cost-based criteria are based on renewals that bring a deteriorating system back into its original condition. There are two types of maintenance available in practice, namely preventive maintenance before failure and corrective maintenance after

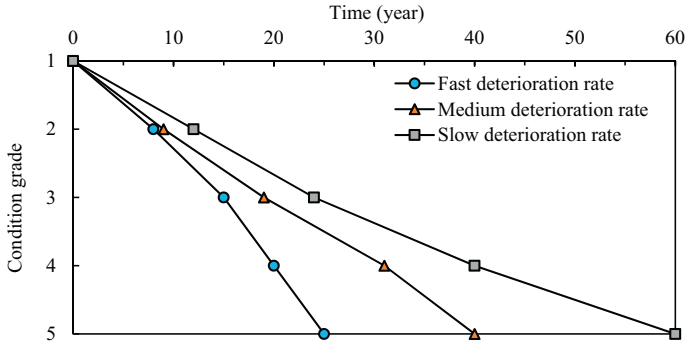

Fig. 7. Typical deterioration rates over time of an earth embankment.

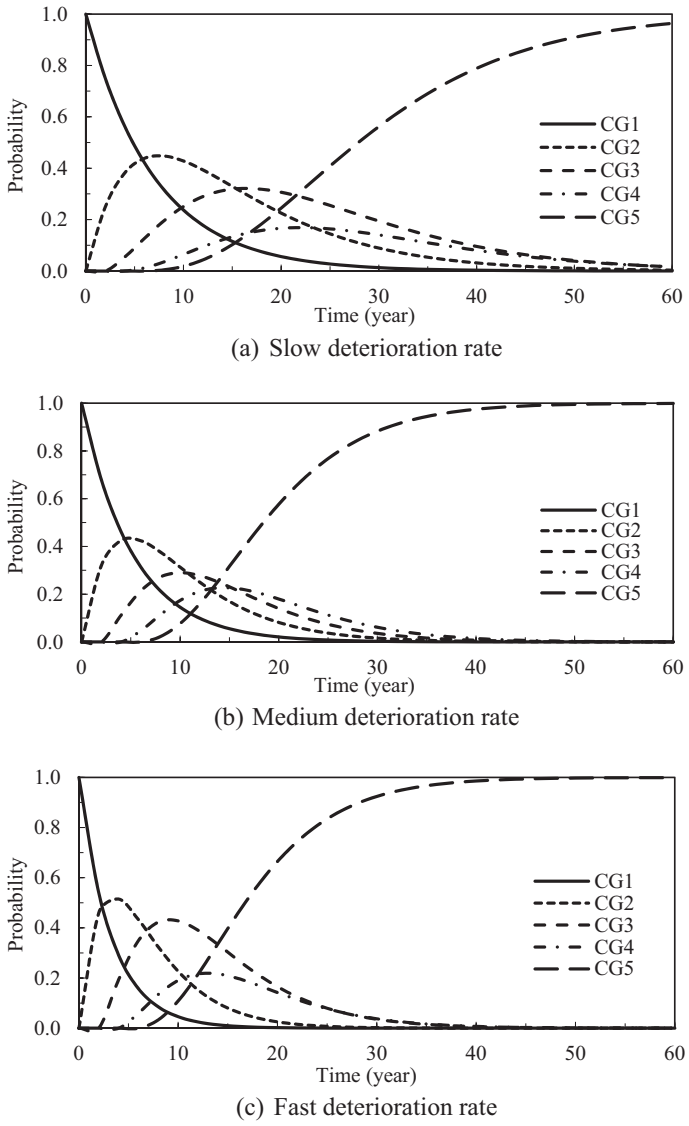

Fig. 8. Time-dependent condition grade (CG) probability distributions during the lifecycle of the earth dyke with various deterioration rates.

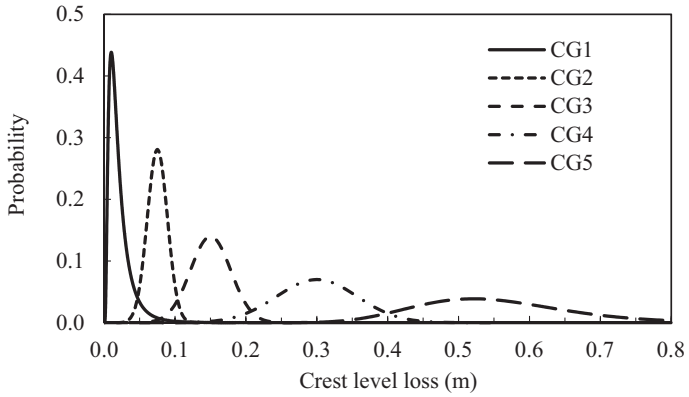

Fig. 9. Probability density functions used for the dyke crest level loss associated with various condition grades (CG).

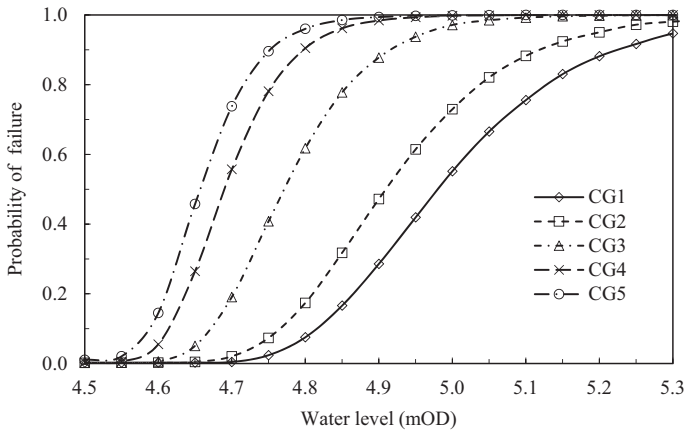

Fig. 10. Wave overtopping fragility curves of the earth dyke under different condition grades (CG) of the dyke crest level loss.

failure. Through timely and effective maintenance the system's deterioration can be delayed and controlled, so that failure of the system is postponed and the system's lifetime is extended.

Maintenance of a coast flood defence can be modelled as a discrete-time renewal process, where the probability of failure per unit time is given in Eq. (20). The optimal maintenance decision can be determined by minimising the long-term average cost per unit time. From the renew reward theory [28], the expected average costs per unit time depend on the preventive maintenance cost C_P and the corrective maintenance cost C_F where $0 < C_P \leq C_F$, expressed here as

$$C_u(k) = \frac{\sum_{i=1}^{k} p_i C_F + (1 - \sum_{i=1}^{k} p_i) C_P}{\sum_{i=1}^{k} i p_i + k(1 - \sum_{i=1}^{k} p_i)} \tag{21}$$

where $k = 1, 2, 3\ldots$ indicates the number of time intervals to be determined by minimising the expected average costs per unit time.

When the future cost is discounted to its present value with a discount factor per unit time $d = (1 + d_r)^{-1}$ in which d_r is discount rate per unit time, the expected discounted costs over time intervals $(0, k)$ are expressed as

$$C_d(k) = \frac{(\sum_{i=1}^{k} d^i p_i) C_F + d^k (1 - \sum_{i=1}^{k} p_i) C_P}{1 - [(\sum_{i=1}^{k} d^i p_i) + d^k ((1 - \sum_{i=1}^{k} p_i))]} \tag{22}$$

The optimal maintenance time interval k^* without and with cost discounting are then determined by minimising the relevant costs given in Eqs. (21) and (22), respectively.

5. Numerical example

A numerical example for an earth sea dyke section shown in Fig. 1 is utilised for analysing the probability of wave overtopping failure of the structure due to rising sea level and crest level loss over time. The earth dyke section is generated from the typical earth embankments of Thames Estuary flood defence systems at Isle of Sheppey, as described in [30]. The earth sea dyke has a crest height of 7.80 mOD and a seaside slope of 1:4. The seaside slope is protected by grass to reduce the destructive effects of sea waves.

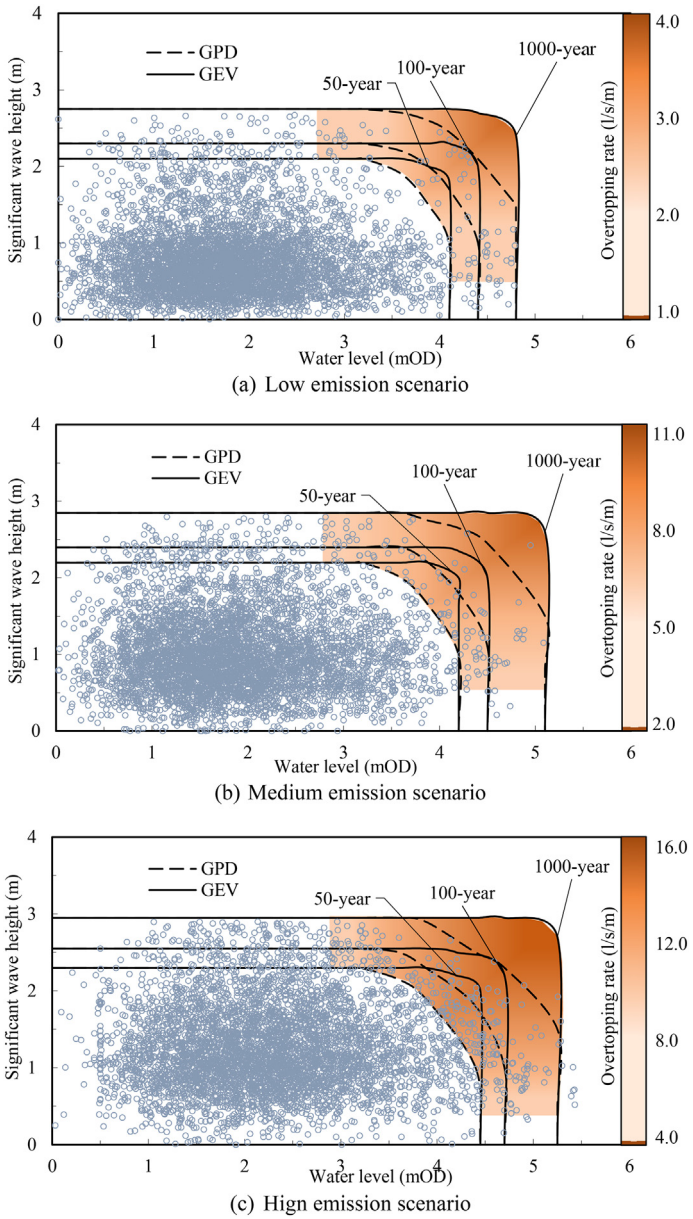

Fig. 11. Joint exceedance for sea water level and significant wave height under different return periods after 60 years subject to medium deterioration rate.

Information on hydraulic parameters such as sea level and wave height is extracted from the data given by UK Environment Agency [31]. Extreme sea levels and significant wave heights from the datasets take into account storm surges and astronomical tide levels at the estuary, and their distributions are then modelled using the GEV and GPD distributions to fit annual maxima.

Fig. 2 gives the results for the mean excesses for sea water levels and significant wave heights at present day with 95% confidence intervals. The mean excesses are plotted for evaluating the expectation of the GPD excesses and for selecting a suitable threshold. From the results, the fitted mean excesses of sea water level appear to have linear relation with respect to the water level up to threshold of 1.15 mOD, while the fitted mean excesses of significant wave height seem to have linear relation with respect to the wave height up to threshold of 0.45 m. After the regions of the linear relations, the fitted curves flutter with respect to sea water level or significant wave height with wider 95% confidence intervals.

The diagnostic plots are provided to check the suitability of the fitted GEV and GPD models to the datasets of sea water levels and significant wave heights, respectively, as shown in Figs. 3 and 4. The probability plot, quantile plot and probability density plot are used for analysing the fit of the GEV and GPD models. The probability plot consists of plotting the theoretical probabilities in function of the empirical model ones to assess whether or not a data set follows the theoretical model such as the GEV or GPD. The quantile

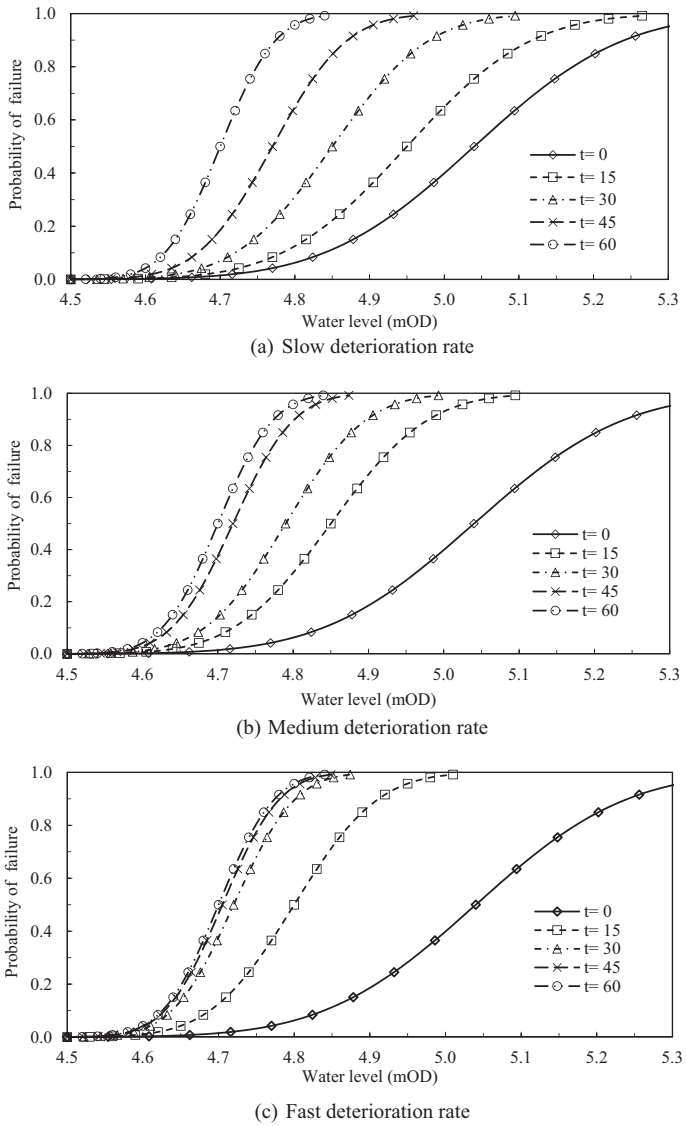

Fig. 12. Wave overtopping fragility curves of the earth dyke at certain time t (years) during the lifecycle subject to various deterioration rates.

plot consists of plotting the theoretical quantiles in function of the observed ones. If the theoretical model adopted is correct, then points should be near the reference line $y = x$ in both probability plot and quantile plot. Departures from this reference line indicate departures from the specified distribution. The probability density plot is used to specify the probability of the random variable falling within a particular range of values, and typically displayed as a histogram consisting of equal-width vertical bars (bins). The theoretical probability density is then plotted as a continuous curve to compare with the histogram.

From the results shown in Fig. 3, both the GEV and GPD models have a good fit to the present water level dataset, since the points of the probability plots and the quantile plots lie close to the unit diagonal. The probability density plots also shows good agreement between the fitted GEV or GPD distribution function and the corresponding empirical density. Furthermore, the GEV fit may be slightly more appropriate for extreme value analysis, since the deviation between the model and the data is less significant for extreme water levels. However, the level of the deviation for the GPD model is not significant, and the original data can be modelled as the GPD distribution with consideration of an appropriate threshold.

As shown in Fig. 4, the comparison between the quantile plots for significant wave height suggests that the GPD model is a more suitable fit for significant wave heights, although both the GEV and GPD models give a good fit from the probability plots. Also, from the corresponding density plots, both the GEV and GPD models show a good fit for the dataset. However, the GEV model tends to give higher extreme values than the GPD model from the quantile plots, and the GPD model may estimate more realistic extreme values for significant wave heights than the GEV model.

Fig. 5 shows the results for the return periods of the GEV and GPD fitted models for hydraulic parameters such as sea water level

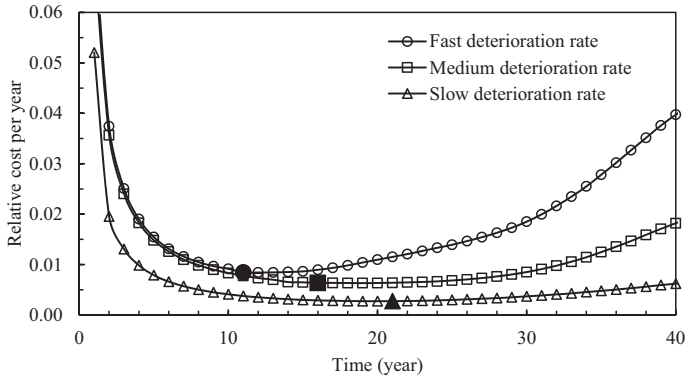

(a) Relative annual costs without discounting

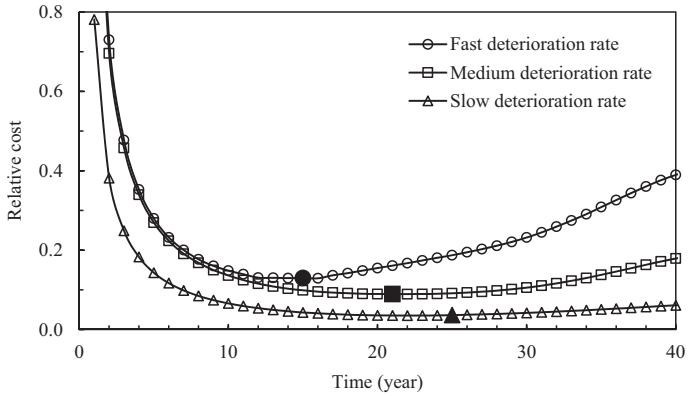

(b) Relative costs with discounting of an annual rate of 5%

Fig. 13. Expected relative costs as a function of time for various dyke crest level deterioration rates.

and significant wave height at present day and after 60 years. The projected sea level rise at the locations around Thames Estuary suggested in UKCP [2] is adopted in calculations, subject to low, medium and high emission scenarios. The foreshore slope of 1:30 is considered with respect to the sensitivity increases in storm surge and offshore wave height. From the results, the estimated extreme values for sea water level at present day at 1000-year return period are 4.63 mOD and 4.52 mOD for the GEV and GPD fitted models, respectively. Both the GEV and GPD fitted models provide very close increases in future water level from the present day, and give approximately water level rise with values of 0.38 m, 0.40 m, 0.32 m at 1000-year return period after 60 years under low, medium and high emission scenarios, respectively. The extreme values for significant wave heights at the present day at 1000-year return period are 2.62 m and 2.50 m for the GEV and GPD fitted models, respectively. Again, both the GEV and GPD fitted models give similar increases in future significant wave heights from the present day. The results of the extreme values of hydraulic parameters in this study are consistent with the results of the extreme values estimated by McMillan et al. [30]. The depth-limited significant wave height at the toe of the earth sea dyke can then be estimated with consideration of the local relative water depth and the foreshore slope [15].

The dependence coefficient between sea water level and significant wave height is estimated for various emission scenarios for the copula function defined in Eq. (7). Monte Carlo simulations are utilised to generate the samples of sea water level and significant wave height. The process for data analysis and simulations includes fitting extreme values to water level and wave height, then transforming each variable from marginal distributions to lognormal distributions, and finally estimating the dependence value by transforming the data into the copula scale using a kernel estimator. From the simulations, the dependence coefficient between sea water level and significant wave height has a value of 0.067.

Fig. 6 shows the results for the joint exceedance for sea water level and significant wave height at present day. The counter lines represent various return periods, e.g. 50, 100 and 1000 years, for sea water levels and significant wave heights generated from the GEV and GPD fitted models. Hear again, the GEV fitted model gives higher extreme values than the GPD fitted model for the same return period, and the GPD fitted data may be closer to the reality. The worst scenario of hydraulic conditions combining sea water level with significant wave height at present data for a 1000-year event is estimated as (4.55 mOD, 2.60 m) for the GEV fitted model and (4.20 mOD, 2.20 m) for the GPD fitted model. The corresponding wave overtopping discharge rate is approximately 1.2 and 0.9 l/s/m for the GEV and GPD fitted models, respectively. Other extreme values close to the above worst hydraulic condition

scenario should also be considered in analysing probability of overtopping failure.

The probability of overtopping failure is also affected by the deteriorating crest freeboard due to settlement of the earth dyke. The earth dyke is assumed in a very good condition (CG1) when it is newly constructed with the initial condition state probability of $\boldsymbol{C_0}$ = [1 0 0 0 0]. Typical deterioration curves with various rates suggested by expert judgment [32] are adopted for modelling the deterioration of the earth dyke, as shown in Fig. 7. These deterioration curves are then utilised to estimate the transition probabilities between the condition grades. A non-linear optimisation method is required to evaluate the transition probability matrix **P** for the optimisation problem defined in Eq. (14) subject to the constraints given in Eq. (12b).

From the obtained transition probability matrix, the probability distribution of the condition grades during the lifecycle of the earth sea dyke is calculated from Eq. (15) for various deterioration rates, as plotted in Fig. 8. The results show how the earth dyke deteriorates from initial condition grade (CG1) to worse condition grades (CG2 to CG5) as age progresses. From the results, the probability of CG1 vanishes at approximately 30, 22, and 13 years from the initial state, subjected to slow, medium and fast deterioration rates, respectively. As expected, the probability of the worst condition grade (CG5) increases steadily with time, reaching probability values of approximately 56%, 82% and 94% at the age of 30 years for slow, medium and fast deterioration rates, respectively.

In order to simulate the crest level loss of the earth dyke, the probability density functions are used for different condition grades, as shown in Fig. 9. The lognormal distribution is adopted for condition grades CG1 and CG5 and the normal distribution is used for condition grades CG2 to CG4. The mean value and standard deviation of the distributions are estimated from the data given in Table 2. The distributions depend on the inspection strategy adopted in the field condition assessment. For example, the accuracy of the inspection data carried out by a trained assessor could be assumed to be 92% (e.g. the remaining 8% wrongly assigned to other condition grades), hence the mean value and standard deviation of the dyke crest level loss are 0.15 m and 0.0285 m for condition grade CG3, respectively.

Fig. 10 gives the results for wave overtopping fragility curves of the earth sea dyke subject to crest level deterioration at various condition grades (CG1 to CG5). The wave overtopping discharge rate is estimated with consideration of reducing crest freeboard due to deteriorating dyke crest level, where the influence factor for slope roughness is taken as $\gamma_f = 0.90$. A critical wave overtopping discharge of 1 l/s per meter length, suggested in [15] for protecting earth dyke crest and landside slope, is adopted in the limit state equation in Eq. (18). A total number of 1×10^5 samples are utilised in the Monte Carlo simulations to estimate the probability of failure. As expected, the fragility curves shift to left when the earth dyke condition becomes worse, e.g. from CG1 to CG5. For example, when the dyke has a water level of 4.80 mOD, the failure probability is approximately 7% at CG1, and increases to approximately 61% at CG3 and approximately 95% at CG5. A maintenance is then necessary to improve the performance of the earth sea dyke by increasing the crest level.

The results in Fig. 11 are given for the joint exceedance for sea water level and significant wave height subject to three emission scenarios for climate change after 60 years. Here, medium deterioration rate is considered for the crest level loss of the earth sea dyke. From the results, the GEV fitted model estimates the worst cases for sea water level and significant wave height of (4.80 mOD, 2.65 m), (5.15 mOD, 2.75 m) and (5.25 mOD, 2.90 m) at 1000-year return period for low, medium and high emission scenarios, respectively. The GPD fitted model gives lower values at the same return period for the worst cases under various emission scenarios. The simulated sea water levels and significant wave heights are then used for calculating wave overtopping discharge of the earth dyke with medium crest level deterioration rate. The extreme overtopping rate under low emission scenario is approximately 4 l/s/m, but increases significantly to 11 and 16 l/s/m under medium and high emission scenarios, respectively.

Fig. 12 shows the results for the wave overtopping fragility curves of the earth sea dyke subject to slow, medium and fast deterioration rates for the crest level loss. Hydraulic conditions affected by climate change with medium emission scenario are considered in estimating wave overtopping discharge, and a critical wave overtopping discharge of 1 l/s per meter length is used in the given limit state equation. The wave overtopping fragility curves are plotted for various ages within the lifecycle, e.g. at 0, 15, 30, 45, and 60 years. From the results, the probability of failure increases steadily with time for all deterioration rates of the dyke crest level loss, and increases more quickly during the beginning of the lifetime when the crest level deteriorates faster. As expected, the crest level loss rate has a significant impact on the probability of overtopping failure. For example, in the case when the earth dyke has serviced for 30 years and water level is at 4.80 mOD, the failure probability is about 24% for slow crest level deterioration rate, but increases to 55% and 91% for medium and fast deterioration rates, respectively.

The risk caused by wave overtopping failure due to sea level rise and dyke crest level deterioration needs to be properly managed, while the costs for the maintenance of the deteriorating sea defences should be minimised. From the renew reward theory, an optimal value of the repair time can be determined by minimising the costs defined in Eqs. (21) or (22) with respect to the number of time interval k. It is assumed here that the corrective maintenance cost $C_F = 1.0$ and the preventive maintenance cost $C_P = 0.05C_F$ for the failure due to excessive wave overtopping, since only relative costs are needed in the calculations. Fig. 13 provides the results for the expected relative costs without and with cost discounting as a function of the repair time for different dyke crest level deterioration rates. The results without cost discounting give optimal repair time at 21 years for slow deterioration rate, but reduced to 16 and 11 years for medium and fast deterioration rates, respectively. In the case with cost discounting of an annual rate of 5%, results suggest the optimal repair times could be delayed 3–5 years for various deterioration rates, comparing with the corresponding optimal repair times for the case without cost discounting.

6. Conclusions

In this study, a method for assessing the time-dependent probability of wave overtopping failure of coastal flood defences during

the lifecycle has been presented. The hydraulic parameters such as sea water level and significant wave height at present day and in the future are investigated with consideration of sea level rise due to climate change. The extreme values of the hydraulic parameters are estimated by analysing extreme values for marginal distributions such as the GEV and GPD distributions. The joint occurrence of sea water level and significant wave height is analysed using joint probability methods. In order to investigate the effect of crest level loss on wave overtopping of sea defences, the state-based stochastic Markov process is introduced to model the deterioration of crest level based on the condition grades obtained from regular inspections. From the limit state equation of wave overtopping failure, the time-dependent probability of failure is calculated with consideration of both changing hydraulic parameters and crest level deterioration over time. The optimal maintenance strategy during the life cycle is then determined by minimising the expected costs associated with maintenance costs and risk of overtopping failure. Finally, a numerical example is given to demonstrate the applicability of the proposed method for assessing the time-dependent reliability of sea defences.

Based on the results for the numerical example involving the earth sea dyke subjected to sea level rise and crest level loss over time, the following conclusions are noted: 1) The rising sea water level due to climate change directly reduces the crest freeboard of the coastal flood defences, and also increases the depth limited significant wave height near the toe, causing double effect on wave overtopping; 2) The performance deterioration of existing sea defences such as crest level loss can be modelled using a state-based stochastic process such as Markov process to translate the condition grades over time from field inspection data; 3) The probability of overtopping failure of existing sea defences during the lifecycle increases significantly due to sea level rise and crest level loss overtime, posing significant risk to the existing coastal flood defences; 4) the risk cost optimised maintenance strategy can be determined by optimising the balance between the costs for structural repairs and the risk of structural failure, depending on deterioration rate, inspection strategy and maintenance costs.

Acknowledgements

The authors are grateful for the financial support from the Natural Environment Research Council (Project No. NE/M008487/1) and the Institution of Civil Engineers through the R & D Enabling Fund (Project No. 1305). The findings and opinions expressed in this study are those of the authors alone and are unnecessarily the views of the sponsors.

References

[1] N. Nakicenovic, J. Alcamo, A. Grubler, K. Riahi, R.A. Roehrl, H.H. Rogner, N. Victor, Special Report on Emissions Scenarios (SRES), A special report of Working Group III of the Intergovernmental Panel on Climate Change (IPCC), Cambridge University Press, 2000.
[2] G. Jenkins, J. Murphy, D. Sexton, J. Lowe, P. Jones, C. Kilsby, UK Climate Projections: Briefing Report Version 2, Met Office Hadley Centre, Exeter, UK, 2010.
[3] A. Arns, S. Dangendorf, J. Jensen, S. Talke, J. Bender, C. Pattiaratchi, Sea-level rise induced amplification of coastal protection design heights, Sci. Rep. 7 (2017) 201–213.
[4] S. Hallegatte, C. Green, R.J. Nicholls, J. Corfee-Morlot, Future flood losses in major coastal cities, Nat. Clim. Chang. 3 (9) (2013) 802–815.
[5] F. Bosello, E. De Cian, Climate change, sea level rise, and coastal disasters: a review of modelling practices, Energy Econ. 46 (2014) 593–605.
[6] P.J. Hawkes, D. Gonzalez-Marco, A. Sánchez-Arcilla, P. Prinos, Best practice for the estimation of extremes: a review, J. Hydraul. Res. 46 (2) (2008) 324–332.
[7] N. Chini, P.K. Stansby, Extreme values of coastal wave overtopping accounting for climate change and sea level rise, Coast. Eng. 65 (2012) 27–37.
[8] H.-P. Chen, Structural Health Monitoring of Large Civil Engineering Structures, John Wiley & Sons Limited, Oxford, UK, 2018.
[9] H.S. Baik, H.S. Jeong, D.M. Abraham, Estimating transition probabilities in Markov chain-based deterioration models for management of wastewater systems, J. Water Resour. Plan. Manag. 132 (1) (2006) 15–24.
[10] D. Saydam, D.M. Frangopol, Y. Dong, Assessment of risk using bridge element condition ratings, J. Infrastruct. Syst. 19 (3) (2012) 252–265.
[11] F.A. Buijs, J.W. Hall, P.B. Sayers, P.H.A.J.M. Van Gelder, Time-dependent reliability analysis of flood defences, Reliab. Eng. Syst. Saf. 94 (12) (2009) 1942–1953.
[12] H.-P. Chen, Maintenance of earth sea dykes in changing environmental and structural conditions, Structural Safety & Reliability, CRC Press, Tokyo, Japan, 2014IALCCE.
[13] H.-P. Chen, Time-dependent reliability analysis of coastal defences subjected to changing environments, Struct Monit Mainten 2 (1) (2015) 49–64.
[14] H.-P. Chen, A.M. Alani, Reliability and optimised maintenance for sea defences, Proc Inst Civil Eng Maritime Eng 165 (2) (2012) 51–64.
[15] J.W. Van der Meer, T. Pullen, N.W.H. Allsop, T. Bruce, A. Kortenhaus, H. Schuttrumpf, EurOtop II: Wave Overtopping of Sea Defences and Related Structures: Assessment Manual, (2016).
[16] M. Masina, A. Lamberti, R. Archetti, Coastal flooding: a copula based approach for estimating the joint probability of water levels and waves, Coast. Eng. 97 (2015) 37–52.
[17] E.B. Santos, P.S. Lucio, C.M.S. Silva, Estimating return periods for daily precipitation extreme events over the Brazilian Amazon, Theor. Appl. Climatol. 126 (3–4) (2016) 585–595.
[18] C. Genest, L.P. Rivest, Statistical inference procedures for bivariate Archimedean copulas, J. Am. Stat. Assoc. 88 (1993) 1034–1043.
[19] Environment Agency, Condition Assessment Manual: Managing Flood Risk, Document Reference 116-03-SD01, Bristol, UK, 2006.
[20] G. Long, M. Smith, M. Mawdesley, A. Taha, Quantitative Assessment Methods for the Monitoring and Inspection of Flood Defences: New Techniques and Recent Developments, CIRIA C717, UK, London, 2013.
[21] M. Pinsky, S. Karlin, An Introduction to Stochastic Modelling, Academic Press, New York, 2010.
[22] J.J. Ortiz-García, S.B. Costello, M.S. Snaith, Derivation of transition probability matrices for pavement deterioration modelling, J. Transp. Eng. 132 (2) (2006) 141–161.
[23] T. Pullen, W. Allsop, T. Bruce, A. Kortenhaus, H. Schuttrumpf, J. Van der Meer, Wave Overtopping of Sea Defences and Related Structure: Assessment Manual, (2007).
[24] J. Van der Meer, Reliability Analysis of Flood Defence Systems, Delft Hydraulics, Report H, Delft, the Netherlands, (1990).
[25] A. Birolini, Reliability Engineering: Theory and Practice, 8, Springer, Heidelberg, 2017.
[26] M.B. Mehrabani, H.-P. Chen, M.W. Stevenson, Overtopping failure analysis of coastal flood defences affected by climate change, J Phy Conf Series 628 (1) (2015) 130–139.
[27] H.-P. Chen, A.M. Alani, Optimized maintenance strategy for concrete structures affected by cracking due to reinforcement corrosion, ACI Struct. J. 110 (2) (2013) 229–238.
[28] J.M. Van Noortwijk, A survey of the application of gamma processes in maintenance, Reliab. Eng. Syst. Saf. 94 (1) (2009) 2–21.
[29] J.M. Van Noortwijk, Explicit formulas for the variance of discounted life-cycle cost, Reliab. Eng. Syst. Saf. 80 (2) (2003) 185–195.
[30] A. McMillan, C. Batstone, D. Worth, J. Tawn, K. Horsburgh, M. Lawless, Coastal Flood Boundary Conditions for UK Mainland and Islands: Design Sea Levels, Project SC060064/TR2 (2011).
[31] Environment Agency, Best Practice in Coastal Flood Forecasting, R&D Technical Report FD2206/TR1, Defra, London, 2004.
[32] Halcrow Group, Practical Guidance on Determining Asset Deterioration and the Use of Condition Grade Deterioration Curves: Revision 1, Environment Agency, Bristol, UK, 2013.